Cement & Concrete Composites 34 (2012) 297–305

Contents lists available at SciVerse ScienceDirect

Cement & Concrete Composites

journal homepage: www.elsevier.com/locate/cemconcomp

Preparation and evaluation of polymer/clay nanocomposite surface treatments for concrete durability enhancement

Paola Scarfato [a,b,*], Luciano Di Maio [a,b], Maria Letizia Fariello [a], Paola Russo [a], Loredana Incarnato [a,b]

[a] Department of Industrial Engineering, University of Salerno, Via Ponte Don Melillo, 84084 Fisciano (SA), Italy
[b] Research Centre NANO_MATES, University of Salerno, Via Ponte Don Melillo, 84084 Fisciano (SA), Italy

ARTICLE INFO

Article history:
Received 1 February 2011
Received in revised form 19 October 2011
Accepted 14 November 2011
Available online 22 November 2011

Keywords:
Concrete
Surface treatments
Nanocomposites
Durability
Transport properties
Porosity

ABSTRACT

In this work, the effectiveness of nanocomposite surface treatments as protective systems for concrete substrates was evaluated. The study was carried out on hybrid organic–inorganic systems prepared by solvent intercalation of an organomodified montmorillonite into two commercial resins: a coating and a pore liner. The obtained nanocomposite systems at 2, 4 and 6 wt% of nanoclay were applied on concrete substrates and characterized to evaluate their protection performances in comparison with the plain resins. In particular, the effect of the different treatments on liquid and vapor water barrier properties, salt attack resistance, porosity, surfaces water repellency and color changes were analyzed. The results demonstrated that the nanoclay addition can significantly improve the protection effectiveness of both the used plain resins, with chromatic modifications undetectable to the naked eye. However, the extent of the obtained gain strongly depends on the chemical nature and therefore on the mechanisms of action of the matrix.

1. Introduction

The unique properties of concrete have determined in the past century its success as a very efficient and adaptable building material. Nevertheless, in the last decades the problem of its long-term performance assurance is gaining a growing interest especially for structures exposed to aggressive environments or severe service conditions, owing to the high costs associated with maintenance and repair operations.

Durability of concrete depends strongly on its pore structure, especially porosity and pore size distribution, and structural detailing: these factors determine the transport properties to the main harmful agents (water, ions and gases) that may cause concrete deterioration by physical and/or chemical attack [1,2].

Nowadays, several strategies are being applied to extend the useful lifetime of structures. In the new construction field, high durability is commonly obtained by means of High Performance Concretes (HPC's), characterized by high strength and low permeability thanks to the use of low water/cement (w/c) ratios and various kinds of admixtures in the formulation [3,4]. Another solution, applicable for protection and also consolidation purposes to both new and existing structures, is the use of polymeric surface treatments or coatings with high barrier properties and hydrophobicity [5,6]. According to their formulation, these treatments have different mechanisms of action and can be classified as: (i) *coatings* and *sealers*, which form a barrier film over the concrete surface (polyurethane, acrylic and epoxy resins); (ii) *pore-liners*, hydrophobic materials that line concrete surface pores and prevent water transport (silane, siloxane and fluorinated polymers); (iii) *pore-blockers*, which penetrate concrete and block pores (liquid silicates and liquid silicofluorides) [7]. A wide range of polymeric surface treatments have been developed in these years: commercialized products include fluorinated, silane and siloxane polymers, acrylic or epoxy resins, and polyurethanes [8–10]. The choice of the most appropriate polymeric treatments depends on the technical and performance requirements [8].

Even if many investigations have demonstrated that surface treatments have the potential to improve significantly the performance of building materials and structures, i.e. by reducing the penetration of the aggressive agents [11–13], enhancing the freeze–thaw resistance [14] or protecting the internal steel reinforcements against corrosion due to chloride diffusion [3,15–17], there is still a need to improve their long-term behavior in typical service environments, to increase their compatibility with the substrates and to further heighten their barrier properties, with the aim to enhance their durability.

On this issue, a new class of surface treatments based on polymeric nanocomposites is recently becoming the subject of investigation, due to the potential benefits that they could offer. It is well known, in fact, that these organic–inorganic materials, in particular the polymer/nanoclay systems, compared to the neat resin are

* Corresponding author at: Department of Industrial Engineering, University of Salerno, Via Ponte Don Melillo, 84084 Fisciano (SA), Italy. Tel.: +39 089 963404; fax: +39 089 964057.
E-mail address: pscarfato@unisa.it (P. Scarfato).

0958-9465/$ - see front matter © 2011 Elsevier Ltd. All rights reserved.
doi:10.1016/j.cemconcomp.2011.11.006

characterized by enhanced mechanical and barrier properties, thermal stability, fire retarding ability, wear resistance, etc., even at low loadings of clay (<6 wt%) [18–21]. However, up to now experimental papers about the possible applications of nanocomposite-based surface treatments in civil engineering and in the conservation and restoration fields are very rare and the acquired knowledge is very far from being systematized [22–28].

In this perspective, we are conducting a study on the effectiveness of nanocomposite surface treatments as protective/consolidating systems for construction building materials. In a previous work we demonstrated the effectiveness of the addition of small amounts (4–6 wt%) of a layered organomodified sodium montmorillonite in increasing the barrier properties to liquid and vapor water and the sulfate attack resistance of a commercial acrylic-fluorinated resin applied on natural tuff stones [25]. On the basis of these results, in the present paper, the study has been extended to the evaluation of the protective ability of nanocomposite treatments towards concrete substrates. In particular, the work has been carried out using nanocomposite systems at several clay contents based on commercial resins with different behaviors: a coating, consisting of a vinylidenefluoride matrix, and a pore liner, consisting of a siloxane matrix. The nanocomposite treatment effectiveness has been evaluated through morphological, physical and colorimetric analyses (SEM, liquid and vapor water transmission, salt crystallization resistance) and correlated to the changes in surface water repellency and porosity of the treated substrates.

2. Experimental

2.1. Materials

2.1.1. Concrete specimens

The concrete for the substrate was produced with a pozzolanic cement designated CEM IV/B 32.5R, which is equivalent to UNI EN 197-1 (2007) requirements. The mixture proportions of the concrete by mass were 1.0 (pozzolanic cement): 2.7 (sand, 2 mm maximum size): 0.5 (fine aggregates, 9.5 mm maximum size): 2.2 (coarse aggregates, 20 mm maximum size) and a water/cement ratio of 0.53. Cubic molds (150 × 150 × 150 mm) were used to obtain the concrete specimens. During the molding of concrete a vibrating needle was used to ensure proper compaction. The molds were removed after 24 h and all specimens were cured for 28 days at 25 °C and 60% R.H.

The samples for testing (cubic specimens 75 × 75 × 75 mm^3 and slabs 75 × 75 × 10 mm^3) were obtained by cutting the cubic concrete blocks by a circular diamond blade saw. Each specimen was brushed on all faces and then subjected to a compressed air jet to remove superficial impurities.

2.1.2. Polymeric resins

Two types of polymeric resins, commercially named as Fluoline CP supplied by CTS S.r.l. (Altavilla Vicentina – VI, Italy) and Antipluviol S supplied by MAPEI S.p.A. (Milano, Italy), were used as protective agents. Fluoline CP is a blend of an acrylic polymer and a vinylidenefluoride based polymer in an acetone solution. It is classified as a coating and is characterized by good reversibility (i.e. it is removable) in acetone. Antipluviol S is a solution based on siloxane resins in a solvent (isooctane/orthoxylene) normally used for exposed concrete structures. It is characterized by a low viscosity which allows the solution to penetrate the concrete pores, thus behaving as a pore liner.

2.1.3. Nanoparticles

The nanoclay, namely Cloisite 30B, was supplied by Southern Clay Products, Inc. It consists of a layered sodium montmorillonite organically modified by N,methyl-N,tallow-N,N′,2-hydroxyethyl-ammoniumchloride (90 meq/100 g clay). Prior to any use, the Cloisite 30B was dried in a vacuum oven at 80 °C for 24 h.

2.2. Methods

2.2.1. Preparation and characterization of polymer–clay nanocomposites

Nanocomposite systems based on Fluoline CP and Antipluviol S resins were obtained at different loadings of Cloisite 30 B (2, 4 and 6 wt%). The required amount of organoclay was first added to the resin with mild stirring until the powder was uniformly dispersed in the resin without any visible agglomerates. The polymer/organoclay mixture was subsequently sonicated for 1 h in an ultrasonic bath (Elma Transsonic 310H) at room temperature to achieve satisfactory dispersion and to promote the exfoliation process of organoclay in the polymeric matrix. Film samples of both the plain resins and their nanocomposites with Cloisite 30B were prepared by solvent casting and tested 7 days after their production.

Film samples are identified as "(X)-30B (wt%)", where (X) is CP for Fluoline CP or AS for Antipluviol S and (wt%) represents the Cloisite loading which refers to 2, 4 or 6 wt%. As received resins are identified as CP or AS.

2.2.1.1. Small angle X-ray diffraction tests. Small angle X-ray diffraction (SAXD) analyses were performed on neat clay powder and nanocomposite films with a Rigaku D/MAX-2000 diffractometer (Ni-filtered Cu Kα radiation, 40 kV, 20 mA). Diffraction scans were collected from 2 to 8 2-theta at a scanning rate of 0.5 deg/min.

2.2.1.2. TEM analyses. Transmission electron microscopy (TEM) analyses on nanocomposite polymeric films were conducted using a Philips EM 208 (acceleration voltage 80 kV). The images were obtained on ultrathin specimens produced with a Leica Ultracut UCT microtome.

2.2.1.3. Thermogravimetric measurements. The thermogravimetric analysis (TGA) on film samples was carried out using a TA Instruments Q500 analyzer, with an increase temperature rate of 10 °C/min under a N_2 atmosphere in the range 25–700 °C. TGA tests were carried out on three replicates of each sample. The mean values of the starting degradation temperature (DTs) and the maximum degradation temperature (DT_{max}) were calculated and reported in Table 1. The standard deviation was always lower than 1.7 °C.

2.2.1.4. SEM analyses. Untreated and treated concrete sample faces were observed by a scanning electron microscope (SEM) model LEO 420 (LEO Electron Microscopy Ltd.). Before analysis, the specimens were sputter coated with 250 Å of a gold–palladium alloy.

2.2.2. Preparation and characterization of treated concrete

Both neat Fluoline CP and Antipluviol S resins as supplied and their mixtures with Cloisite 30B were applied on concrete samples by paint-brushing, according to the procedure recommended in the technical sheet for the neat resin. The average amount of product applied on concrete specimens, determined by weighing the dry samples before and after their treatment, was about 33.0 ± 0.9 g/m^2 for the Antipluviol S-based systems and 24.4 ± 0.8 g/m^2 for the Fluormet CP-based ones. Before testing, in order to evaporate the solvent, all treated samples were dried at room temperature until constant weight was reached ($\Delta M \leqslant 0.001$ g). Observing by the naked eye the treated surfaces, no morphological change is detectable.

Treated concrete specimens are identified as "CLS + (X)-30B (wt%)", where CLS is the acronym for concrete, (X) is CP for Fluoline CP or AS for Antipluviol S and (wt%) represents the Cloisite loading which refers to 2, 4 or 6 wt%.

Table 1
Starting degradation temperature (DT_s) and maximum degradation temperature (DT_{max}) of neat and nanocomposite film samples.

Organoclay amount (%)	CP-based systems		AS-based systems	
	DT_s (°C)	DT_{max} (°C)	DT_s (°C)	DT_{max} (°C)
0	327	424	334	395
2	341	437	365	402
4	350	435	371	408
6	362	433	379	406

2.2.2.1. Water vapor transmission and capillary sorption measurements. Water vapor transport properties of concrete were evaluated at 23 °C by vapor transmission tests according to the water method specified in ASTM E 96/E 96 M – 05, in which a water vapor pressure gradient is applied through the thickness of a concrete plate specimen (untreated or treated on one surface) and the moisture transmission rate is determined. Test dishes were prepared by sealing the specimens to the dishes in such a manner that the dish mouth (having a diameter of 70 mm) defines the area of the specimen exposed to the vapor pressure in the dish. The dishes contain distilled water to a level 19 ± 6 mm from the specimen. They are weighed at certain time intervals in order to determine the rate of vapor transport through the specimen from the water (in the dish the R.H. is nominally 100%) to the controlled atmosphere of a climatic chamber (R.H. 5%, 1 atm). The water vapor transmission rate (WVT, defined as the amount of vapor flowing in unit time through the surface unit of the sample) is calculated by the following equation:

$$\mathrm{WVT} = \frac{\Delta M}{t \cdot A} \tag{1}$$

where WVT is the water vapor transmission rate, ΔM is the steady-state weight change (g), A is the exposed area to water vapor (mm^2) and t is the testing time (s). Samples thickness was 10 mm and the vapor exposed area was 3850 mm^2. The weight loss of the dish assembly (i.e. the water vapor which crosses the specimen) was recorded at intervals of 24 h and the measurement was continued until a steady state weight loss rate had been reached. Vapor transmission tests were carried out on five replicates of each sample.

The measurement of water capillary sorption, according to the UNI EN 1015-18:2004 standard [29] was performed by exposing cubic specimens ($75 \times 75 \times 75$ mm^3) to liquid water on one of the plane ends and by measuring, as a function of time, the weight increase resulting from absorption of water. Specimens (untreated or treated on one base and on all the adjacent lateral surfaces up to a height of 10 mm) were placed in a pan where they were immersed in water at a depth of 5–7 mm for the duration of the experiment. The amount of fluid absorbed was then calculated and normalized by the cross-section area (75×75 mm^2) of the specimen exposed to the liquid. The capillary water uptake typically fits the following equation [30]:

$$\frac{W}{A} = C_{W,S} \cdot \sqrt{t} \tag{2}$$

where W is the mass of water absorbed (kg), A is the exposed area (m^2), t is the time (min) and $C_{w,s}$ is the sorptivity coefficient. Water capillary sorption tests were carried out on five replicates of each sample.

2.2.2.2. Contact angle measurements. Static contact angle measurements were performed with a contact angle system FTA 1000 instrument (First Ten Angstroms, Inc.). Tests were carried out on untreated and treated concrete samples. The contact angles were recorded immediately after the droplets touched the substrate and the reported values are the average of at least five measurements conducted for each test.

2.2.2.3. Sulfate attack tests. Sulfate attack tests were performed according to the ASTM C88-05 (2005) procedure with some adaptations. It consists of cycles of immersion in a saturated solution of sodium sulfate (Na_2SO_4) and drying in an oven at 110 °C to constant weight. The immersion duration was not less than 16 h and no more than 18 h. The volume of the solution was at least five times the volume of the immersed specimens ($75 \times 75 \times 75$ mm^3).

The evaluation of concrete behavior to sulfate attack is then made by measuring the weight variation of the concrete samples (both untreated or treated on all faces) after a total of eight cycles. Only for the coated specimens, due to the low heat resistance of polymeric resins, the drying temperature was set at 75 ± 5 °C [11]. sulfate attack tests were carried out on five replicates of each sample.

2.2.2.4. Mercury intrusion porosimetry measurements. The pore structure of the concrete samples was investigated by a mercury intrusion porosimetry technique with Pascal 140 and Pascal 240 (Thermo Finnigan) instruments. The pressure range of the porosimeters was from sub ambient up to 200 MPa, covering the pore diameter range from about 0.0075 to 100 μm. Thus, the pressure is sufficient to ensure intrusion of mercury in all the capillary pores, as the reported diameter of the smallest size capillary pores is 0.01 μm [31], whereas the majority of the gel pores would remain not intruded. Values of 141.3° and 480 dyne/cm were used for the contact angle and mercury surface tension, respectively. Tests were carried out on small-cored samples with dimensions $20 \times 10 \times 10$ mm^3 taken out from untreated concrete cubes ($75 \times 75 \times 75$ mm^3). The samples were treated on all faces using the same procedure described in 2.2.2 paragraph, thus obtaining coating/concrete volume ratios of about 1/30,000. The samples were dried in an oven at 60 °C overnight and stored in a desiccator until testing. Mercury intrusion porosimeter tests were carried out on five replicates of each sample to ensure adequate accuracy of the results (about 15%).

From mercury intrusion porosimetry data it is also obtained a measure of the total porosity (%) in the sample as that corresponding to the volume of mercury intruded at the maximum experimental pressure divided by the bulk volume (inverse of bulk density) of the unintruded sample.

2.2.2.5. Colorimetric analysis. Colorimetric analysis was carried out on the untreated and treated concrete samples with a CR-410 HEAD colorimeter (Konica Minolta Sensing, Inc.), following the Italian Recommendation NORMAL 43/93 (1993), in order to determine the variation of the aesthetical properties induced by the treatments. Each test was performed making five measurements on each specimen; in order to verify the reproducibility of the results, the test was repeated on three identical specimens, therefore the results reported were the average values of 15 measurements (standard deviations were about 15%). The color changes were evaluated by the L^*, a^*, b^* system (ASTM D-1925, CIE 1976). L^* is the surface lightness and ranges from 0 (corresponding to black) to 100 (corresponding to white); a^* is the coordinate of chromaticity from green (−60) to red (+60) and b^* is the coordinate from blue (−60) to yellow (+60). The total color variation is expressed by ΔE that is calculated as follows:

$$\Delta E = \sqrt{\Delta a^{*2} + \Delta b^{*2} + \Delta L^{*2}} \tag{3}$$

3. Results and discussion

3.1. Resins characterization

In order to verify that the Cloisite 30B lamellar clay was dispersed on a nanometric scale into the polymeric resins, small angle X-ray diffraction (SAXD) measurements were carried out both on

the pristine silicate and on all Fluoline CP and Antipluviol S cast films at different organoclay contents (2 wt%, 4 wt% and 6 wt%). The SAXD profiles are reported in Fig. 1. As can be seen, the Cloisite 30B diffractogram shows the characteristic basal reflection of the neat organoclay centered at about $2\theta = 4.9°$, corresponding to a d-spacing of 1.8 nm. Only in the SAXD profile of the CP-30B 2% sample is this peak still present, but strongly broadened and dampened; however, in this diffractogram a shoulder also grows up at lower 2θ angles, indicating that a partial intercalation of the polymer chains between the silicate layers is occurring (d-spacing > 3.0 nm). In the diffractograms of all the other films, the Cloisite 30B basal reflection completely disappears, suggesting that it has shifted to a 2θ angle below 2° (which is the instrument limit) and therefore that the polymeric resins have successfully intercalated/exfoliated the layered nanofiller.

With the aim to better evidence the hierarchical structure of the hybrids, TEM measurements were carried out on the hybrid films. As an example, Fig. 2 reports the TEM image of the CP-30B 4% system. The image shows that the clay particles, appearing as dark gray lines in the micrograph, are quite homogenously distributed into the CP matrix and really dispersed on a nano-scale; a mixed exfoliated/intercalated morphology was obtained, as demonstrated by the presence of both (i) completely delaminated and individually dispersed silicate sheets and (ii) intercalated structures with small stack dimensions (<15–20 nm), resulting from an extensive penetration of the resin between the Cloisite 30B organoclay layers. A similar nanostructure is also exhibited by the other hybrid films. This kind of morphology, characterized by a high aspect ratio of the nanofiller, is the key factor for the property improvement (heat resistance, barrier and mechanical properties, etc.) typical of polymer-silicate nanocomposites at low particle loadings [18–21].

The effect of the obtained nanoscale dispersion of the Cloisite 30B on the thermal behavior of the nanocomposite polymeric systems was investigated by means of TGA analyses, whose results are reported in Table 1. As it can be seen, both the starting decomposition temperature (DT_s) and the maximum decomposition temperature (DT_{max}) were improved in the nanocomposites. The effect is significant even at the lowest silicate loading and further increases with the filler content. In particular, the DT_s values rise by 35 °C and 45 °C for the CP-30B-6% and AS-30B-6% films, respectively. According to other authors [32,33], the enhancement of the overall thermal stability of the nanocomposite systems can be explained considering that the nanodispersed clay acts as a heat barrier. Thereby, the clay accumulates and holds the heat that could be used as a source to accelerate the decomposition processes, thus shifting the decomposition temperatures to higher values during a dynamic scan.

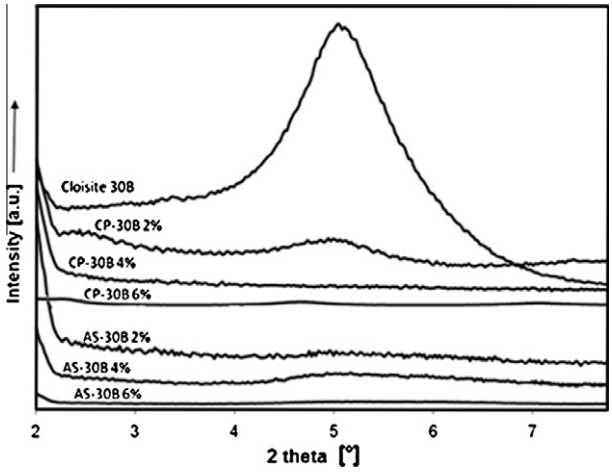

Fig. 1. SAXD of film samples of all plain and nanocomposite polymeric treatments.

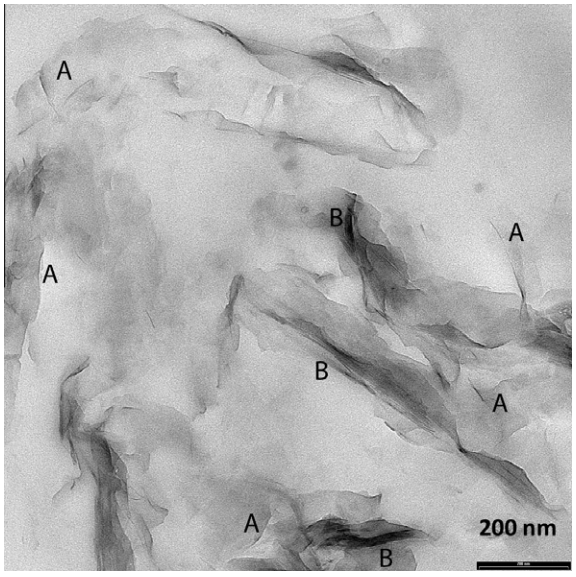

Fig. 2. TEM image of the CP-30B 4% film. A: delaminated silicate sheets; B: intercalated silicate structures.

3.2. Treated concrete characterization

In order to evaluate the protective effectiveness of the nanocomposite treatments, all the systems were applied on the concrete specimens and subsequently tested. Untreated concrete samples, used as control, and treated concrete samples were first observed by SEM, with the aim to analyze the changes in their surface morphology, and afterwards submitted to WVT, capillary sorption and contact angle measurements, sulfate attack resistance tests, porosimetric and colorimetric analyses.

Typical SEM micrographs of concrete surfaces, taken before and after polymeric treatment applications, are reported in Fig. 3a–e. The images clearly show that the Fluoline CP coating forms a film on the plain concrete surface, whereas the Antipluviol S pore liner does not significantly modify the substrate morphology, as expected. The addition of the nanodispersed layered clay to the polymeric resins improves their void coverage ability (even if sometimes pin-holes can be observed in the case of the Fluoline CP nanocomposite coatings) since the nanofiller lamellae tend to arrange themselves parallel to the concrete surface so partially closing up the pores. Consequently, the pore number and size and the surface area exposed to the environment for absorption or permeation of liquids or gases into the concrete are effectively reduced compared to both the untreated concrete and the concrete treated with the plain resins. This leads us to hypothesize that the nanocomposite treatments will have a higher protective effectiveness than the original ones.

The moisture barrier properties of the resins and their nanocomposites at different clay contents were studied by performing water vapor transmission (WVT) tests on untreated concrete, used as a control, and on all treated concrete samples. Fig. 4a and b compare the weight variation against the elapsed test time for the concrete samples untreated or treated with the Fluoline CP (a) and the Antipluviol S-based systems (b). It is evident that both the plain resins do not influence significantly the water vapor transmission behavior, whereas all the nanocomposite systems slow down the phenomenon to an extent that increases with the silicate percentage. In order to better quantify the effect of the different treatments, the WVT rate was calculated from the curves of Fig. 4a

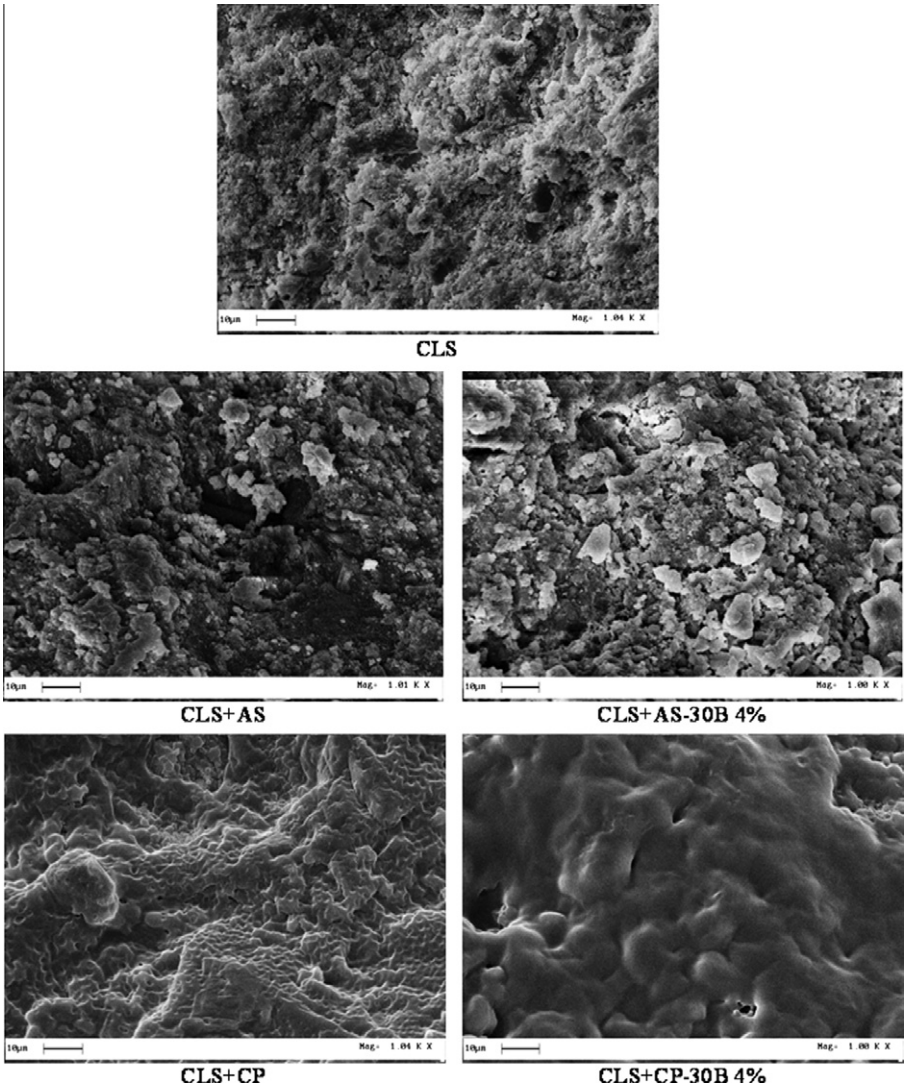

Fig. 3. SEM images of concrete untreated and treated with both neat resins and their nanocomposite blends at 4 wt%.

and b, according to the eq. (1). The data reported in Table 2 confirm that the concrete samples, either untreated or treated with the plain resins, have the highest WVT rate values, similar to one another. On the other hand, the nanocomposite systems produce a decrease of the WVT rate up to approximately 30%, thus enhancing the barrier properties of the treated substrate without preventing its breathing. The result is clearly related to the platelet structure of the clay nanoparticles that increase the tortuosity of the path for the diffusion of the water vapor (and other gases or liquid penetrants) throughout the nanocomposite [34] and partially close up the pores of the concrete, reducing its surface area, as confirmed also by the SEM observations.

In order to verify if and how the clay nanoparticles can also modify the resistance of the treated concrete substrate to the penetration of liquids, water capillary absorption tests and sulfate attack tests were carried out. These kinds of analyses give essential information to evaluate the concrete durability because of the fundamental role of the capillary action in the transport by which aggressive ions such as sulfates and chlorides enter the concrete. Actually, while the primary transport mechanisms are both diffusion and capillary action, diffusion alone can be a very slow process. Hence, it may be the capillary transport, especially near an unsaturated concrete surface, that is the dominant invasion mechanism [30].

Fig. 5 compares the results of the capillary absorption tests performed on concrete samples either untreated or treated with the plain and nanocomposite resins at 4 wt% of clay. In all the absorbed water curves, a short and a long time water absorption stage consistent with a $t^{1/2}$ behavior can be identified, but the sorptivity, $C_{w,S}$ (slope of the curve), is significantly different in the two regimes. In particular, $C_{w,S}$ is higher in the early-time regime in the case of the concrete untreated and treated with the CP-based systems, whereas it is significantly lower for the concrete treated with the AS-based systems.

The first behavior, commonly observed during capillary liquid absorption into porous substrates [35–37], can be justified assuming that the sorption process is dominated at early times by the finer pores, where strong capillary forces greater than gravitational forces act, and at later stages by the coarse pores, where the capillary suction is weaker. However, it is quite possible that, at later stages, the ingress of water into the gel pores limits the rate of flow as well.

The latter behavior, instead, found also in hydrophobic porous substrates [17,37], can be justified assuming that the AS-based treatments make the concrete surface somewhat water repellent. The change in the wettability concerns primarily the walls of the large pores, while the smaller pores are not much affected, because of the high molecular weight of the polymer. Consequently, the

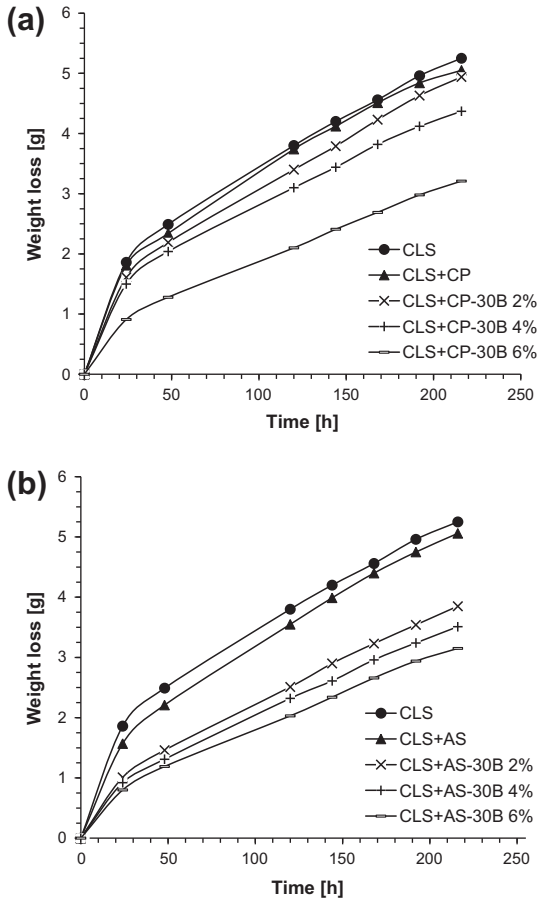

Fig. 4. Weight loss of concrete samples dishes treated with: (a) Fluoline CP and its nanocomposite blends with Cloisite 30B, and (b) Antipluviol S and its nanocomposite blends with Cloisite 30B.

Table 2
WVT rate (g/h m^2) of concrete samples either untreated and treated with the plain and nanocomposite polymeric systems.

Sample	WVT rate ± SD (g/(h m^2))
CLS (control sample)	4.32 ± 0.17
CLS + CP	4.26 ± 0.17
CLS + CP-30B 2%	4.39 ± 0.18
CLS + CP-30B 4%	3.67 ± 0.15
CLS + CP-30B 6%	3.02 ± 0.16
CLS + AS	4.47 ± 0.19
CLS + AS-30B 2%	3.70 ± 0.17
CLS + AS-30B 4%	3.43 ± 0.18
CLS + AS-30B 6%	3.09 ± 0.16

water can enter only very slowly through the treated face of the substrate because only the smaller pores are able to transport it without significant filling of the larger pores in the early time of the experiment. Only at the late-stage of the test some large pores may be partially filled by water and contribute to its absorption by capillary suction.

The curves of Fig. 5 show also that, irrespective of the water absorption behavior, both the plain AS and CP resins significantly reduce the amount of absorbed water compared to the untreated substrate. The effect is further magnified when the nanocomposite treatments were applied, as expected. In fact, as already observed in the case of WVT experiments, the addition of layered nanoclay

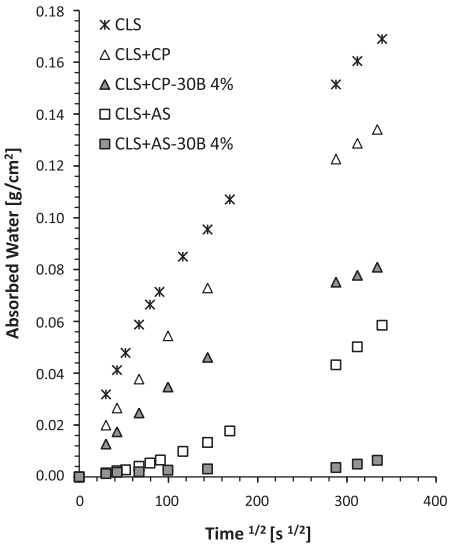

Fig. 5. Cumulative capillary absorption curves of concrete untreated and treated with both neat resins and their nanocomposite blends at 4 wt%.

Table 3
Static contact angle of concrete samples either untreated and treated with the plain and nanocomposite polymeric systems.

Sample	Static contact angle ± SD (deg)
CLS (control sample)	33 ± 3
CLS + CP	84 ± 3
CLS + CP-30B 2%	87 ± 2
CLS + CP-30B 4%	80 ± 2
CLS + CP-30B 6%	76 ± 2
CLS + AS	96 ± 3
CLS + AS-30B 2%	103 ± 2
CLS + AS-30B 4%	104 ± 4
CLS + AS-30B 6%	101 ± 5

particles to the polymeric resins not only improves the barrier properties of the matrices, but also contribute to the pore blockage of the concrete surface.

In order to investigate the effect of the polymeric treatments on the concrete surface hydrophobicity, static contact angle measurements were performed using water as the test liquid. The obtained results are listed in Table 3. The data demonstrate that the application of any of the protective systems produces a drastic increase of the contact angle values compared to the untreated substrate. In particular, the strong hydrophilic character of the concrete becomes

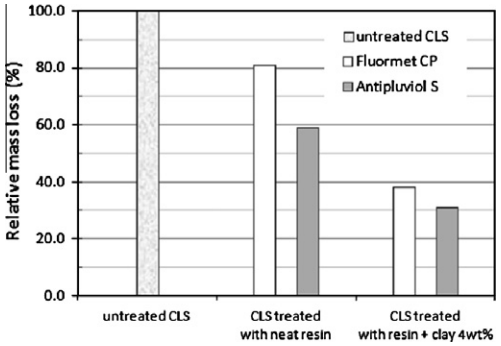

Fig. 6. Relative mass loss after eight cycles of sulfate attack of concrete untreated and treated with neat or nanocomposite resins at 4 wt% of clay.

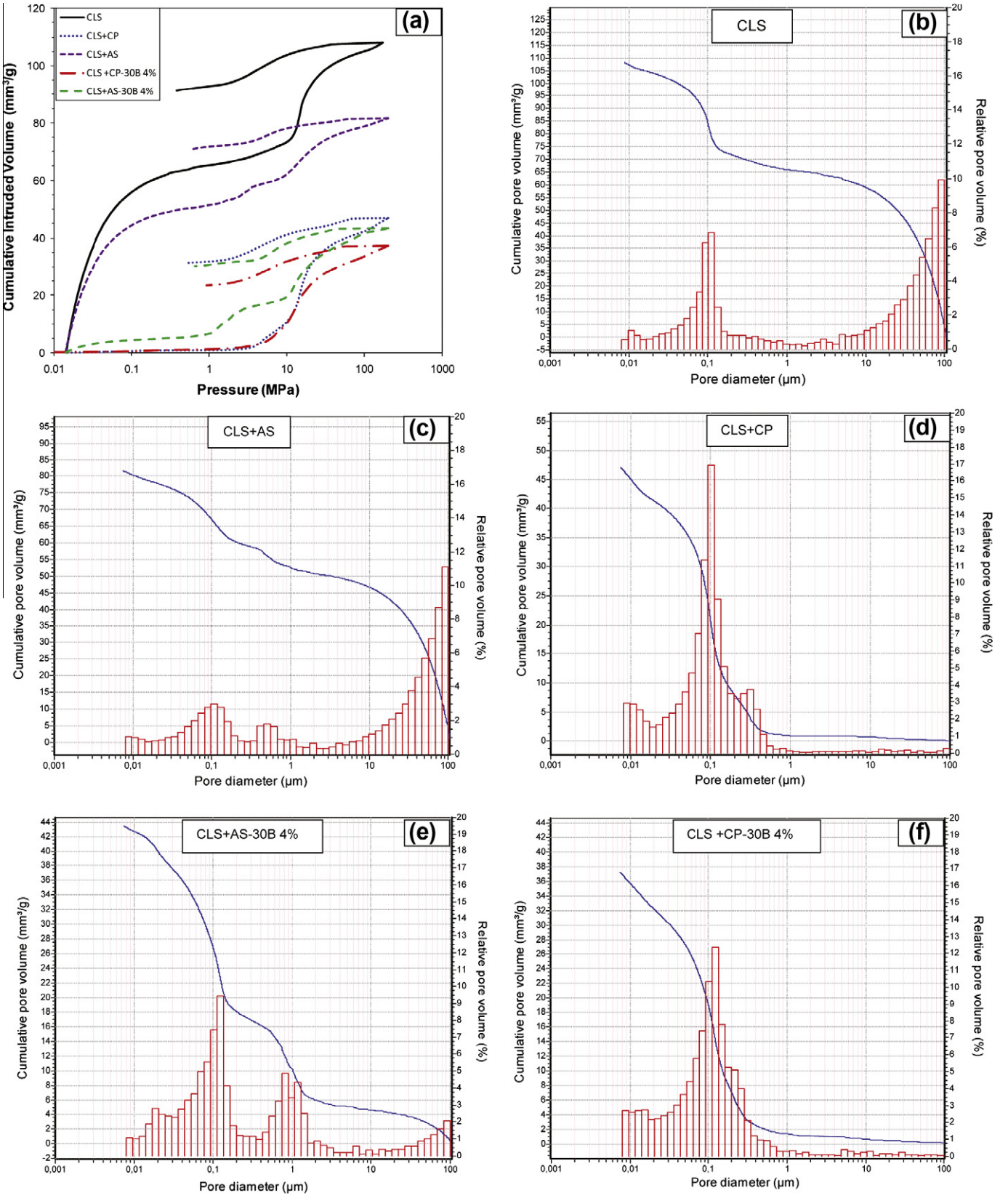

Fig. 7. (a) Cumulative pore volume and b–f) pore size distribution of samples, (b) plain concrete (CLS), (c) CLS + AS, (d) CLS + CP, (e) CLS + AS-30B + 4%, and (f) CLS + CP-30B 4%.

only slightly hydrophilic (near 90°) with the CP-based systems and even slightly hydrophobic with AS-based ones, respectively. These changes are coherent with the capillary absorption curves above discussed.

The results of Table 3 also indicate that the organoclay addition to the polymeric resins produce a slight decrease of the contact angles in the case of the CP-based treatments and a slight increase in the case of the AS-based ones. In regard to this, it is worthy to note

that the nanofiller has a hydrophilic character, thus its presence into the treatment formulations can increase their water wettability, as observed in the case of the CP-based systems. In the case of the AS-based systems this effect may be counterbalanced by the higher surface roughness of the specimens treated with the pore liner [38], as demonstrated by the SEM images (see Fig. 3).

Fig. 6 shows the effect of both the plain and nanocomposite treatments at 4 wt% of clay on the sulfate attack resistance of the concrete. The results are expressed in terms of relative mass losses% (i.e. mass loss of treated specimen/mass loss of untreated specimen x 100) at the end of eight cycles of immersion in a saturated solution of sodium sulfate followed by oven drying to constant weight. The histogram demonstrates the good protective action of all the treatments against the sulfate attack, as predictable on the basis of the capillary absorption and contact angle values reported above. In fact, since the sulfate ion solution penetrates the concrete by capillary suction, the improvement in the concrete surface hydrophobicity due to the treatment application significantly reduces the material deterioration. The protective effectiveness is generally higher for the AS-based systems that exhibit higher contact angle values. Again, the additional beneficial effects of the nanoclay on the sulfate attack resistance can be explained in terms of both an increase of nanocomposite barrier properties and a decrease of the substrate porosity.

Results of mercury intrusion porosimetry are reported in Fig. 7 in terms of cumulative intruded volume of Hg as a function of pressure (Fig. 7a) and as a function of pore diameter (lines in Fig. 7b–f) with pore size distribution of concrete samples (histograms in Fig. 7b–f).

Fig. 7a shows that the Antipluviol S treatment, which is a pore-liner, reduces the Hg intruded volume and, hence, the porosity of plain concrete from 21.0% to 17.7%, while the Fluoline CP one, which is a coating, produces a higher decrease in porosity up to a value of 11.0% (Table 4). The addition of 4%wt clay further decreases the porosity of both the CLS + AS-30B 4% and CLS + CP-30B 4% samples for which a porosity of 10.0% and 8.7%, respectively, was measured (Table 4).

With respect to pore size distribution, the complex pore structure of concrete is evidenced in Fig. 7b, where a bimodal distribution with a first peak at a pore diameter of about 0.1 μm (capillary pores) and a second peak at values ⩾ 100 μm (macropores) were found. This pore structure is greatly influenced by the application of the surface treatments and their nature. The pore liner Antipluviol S affects the substrate pore structure reducing the relative volume fractions of both the macropores (in the range 10–100 μm) and the capillary pores; in particular, for the latter it can be observed a further peak centered at 0.5 μm (Fig. 7c), deriving from the macropores narrowed by the liner resin. On the contrary, the Fluoline CP coating plugs the macropores and significantly decreases the capillary pore volume. Finally, the clay addition influences the pores size distribution of CLS + AS-30B 4%, reducing significantly the fraction of macropores, but it does not affect the pore size distribution of CLS + CP-30B 4%. However, in both cases a slight decrease of the cumulative pore volume can be noticed. These results confirm the ability of the clay to block the pores on the concrete surface, as hypothesized on the basis of the WVT data. Moreover, the reduction of the capillary pore volume of plain concrete observed with both the AS-based and CP-based treatments, significantly higher for the first, agrees with the differences in the capillary water absorption behaviors reported in Fig. 5.

Table 4
Effect of plain and nanocomposite polymeric treatments on the volumetric porosity of the concrete.

Sample	Porosity (%)
CLS	21.0
CLS + CP	11.0
CLS + AS	17.7
CLS + CP-30B 4%	8.7
CLS + AS-30B 4%	10.0

Table 5
Color variation of concrete surfaces either untreated and treated with the plain and nanocomposite polymeric systems.

Samples	ΔL^*	Δa^*	Δb^*	ΔE
CLS	0	0	0	0
CLS + CP	−1.6	0.1	0.1	1.6
CLS + CP-30B 2%	−1.4	0.1	0.1	1.4
CLS + CP-30B 4%	−0.9	0.0	−0.1	0.9
CLS + CP-30B 6%	−0.4	0.1	−0.1	0.5
CLS + AS	−4.3	0.2	0.9	4.2
CLS + AS-30B 2%	−4.0	0.2	0.6	4.1
CLS + AS-30B 4%	−4.0	0.1	0.6	4.0
CLS + AS-30B 6%	−3.5	0.1	0.6	3.5

Finally, the aesthetic alteration of the treated concrete samples was analyzed by means of colorimetric measurements. The values of the ΔL^*, Δa^*, Δb^* and ΔE parameters are listed in Table 5. The protective resins produce a very slight color variation of the treated concrete surfaces. The alteration in the appearance essentially results in a modest variation of the brightness differences ΔL^* while the values of a^* (chromatic parameter from green to red) and b^* (chromatic parameter from blue to yellow) appear not to be or are only slightly affected by the treatments with the polymeric resins and are not related to the clay content. On the whole, the chromatic differences, ΔE are in all cases very small and undetectable to the naked eye.

4. Conclusions

Concrete surface treatments with nanocomposite systems were assessed with regard to the evaluation of transport properties, sulfate attack resistance, porosity, hydrophobicity and color variations. In particular, the protective action of two different commercial polymeric resins was enhanced by dispersing, on a nanoscale, small amounts (2, 4 and 6 wt%) of an organomodified sodium montmorillonite (Cloisite 30B) without any detectable detrimental effect on the chromatic appearance of the treated substrates. In fact, the reported experimental data show that the barrier properties to water vapor remain basically unchanged after the application of the plain resins, whereas they increase by up to 30% using the nanocomposite systems loaded with 6 wt% of clay. These results demonstrate the efficacy of the lamellar nanofiller in improving the moisture penetration resistance of the treated substrate through the pore blockage of the concrete and the lowering of the diffusion properties of the polymer matrices. Concerning the water capillary sorption behavior, it appears strongly dependent on both the character of the resins (hydrophilic or hydrophobic, coating or pore liner) and the nanoclay addition. Best performances have been obtained with the AS-based nanocomposite systems: their hydrophobic nature and pore liner ability, joined with the pore blockage action of the nanoclay, drastically reduce the capillary suction, therefore the water can enter only very slowly and in small quantities through the treated face of the substrate. Of course, this beneficial effect influences positively the sulfate attack resistance, too.

All the changes in the transport behavior of the concrete substrates treated with the different plain and nanocomposite polymeric systems are in accordance with the changes in the surface

water repellency and in the pore size distributions of the samples. The contact angle tests and the mercury intrusion porosimetry measurements, in fact, demonstrate that the CP-based systems are the most effective in reducing the pore volume of the substrate since they coat almost all macropores and partially the capillary pores, but their coatings are slightly hydrophilic; on the other hand, the AS-based systems are less effective in reducing the pore volume, but they shift the pore size distributions towards lower pore diameters and line the pore walls with a slightly hydrophobic polymeric layer.

References

[1] Glasser FP, Marchand J, Samson E. Durability of concrete – degradation phenomena involving detrimental chemical reactions. Cem Concr Res 2008;38:226–46.
[2] Bertolini L, Elsener B, Pedeferri P, Polder R. Corrosion of steel in concrete: prevention, diagnosis, repair. Weinheim: Wiley-VCH; 2004.
[3] Nawy EG. Fundamentals of high performance concrete. 2nd ed. New York: John Wiley and Sons; 2001.
[4] Tittarelli F, Moriconi G. The effect of silane-based hydrophobic admixture on corrosion of reinforcing steel in concrete. Cem Concr Res 2008;38:1354–7.
[5] Vacchiano CD, Incarnato L, Scarfato P, Acierno D. Conservation of tuff-stone with polymeric resins. Constr Build Mater 2008;22:855–65.
[6] Ferreira Pinto AP, Delgado Rodrigues J. Stone consolidation: the role of treatment procedures. J Cultural Heritage 2008;9:38–53.
[7] Levi M, Ferro C, Regazzoli D, Dotelli G, Lo Presti A. Comparative evaluation method of polymer surface treatments applied on high performance concrete. J Mater Sci 2002;37:4881–8.
[8] Basheer PAM, Basheer L, Cleland DJ, Long AE. Surface treatments for concrete: assessment methods and reported performances. Constr Build Mater 1997;11(7–8):413–29.
[9] Tittarelli F. Oxygen diffusion through hydrophobic cement-based materials. Cem Concr Res 2009;39:924–8.
[10] Delucchi M, Barbucci A, Cerisola G. Study of the physico-chemical properties of organic coatings for concrete degradation control. Constr Build Mater 1997;11(7–8):365–71.
[11] Aguiar JB, Camoes A, Moreira PM. Coating for concrete protection against aggressive environments. J Adv Concr Technol 2008;6(1):243–50.
[12] Nolan E, Basheer PAM, Long AE. Effects of three durability enhancing products on some physical properties of near surface concrete. Constr Build Mater 1995;9(5):267–72.
[13] Dai J-G, Akira Y, Wittmann FH, Yokota H, Zhang P. Water repellent surface impregnation for extension of service life of reinforced concrete structures in marine environments: the role of cracks. Cem Concr Compos 2010;32:101–9.
[14] Basheer L, Cleland DJ. Freeze-thaw resistance of concretes treated with pore liners. Constr Build Mater 2006;20:990–8.
[15] Seneviratne AMG, Sergi G, Page CL. Performance characteristics of surface coatings applied to concrete for control of reinforcement corrosion. Constr Build Mater 2000;14:55–9.
[16] Medeiros M, Helene P. Efficacy of surface hydrophobic agents in reducing water and chloride ion penetration in concrete. Mater Struct 2008;41:59–71.
[17] de Vries J, Polder RB. Hydrophobic treatment of concrete. Constr Build Mater 1997;11(4):259–65.
[18] Choudalakis G, Gotsis AD. Permeability of polymer/clay nanocomposites: a review. Eur Polym J 2009;45:967–84.
[19] Pavlidou S, Papaspyrides CD. A review on polymer–layered silicate nanocomposites. Prog Polym Sci 2008;33:1119–98.
[20] Russo GM, Simon GP, Incarnato L. Correlation between rheological, mechanical, and barrier properties in new copolyamide-based nanocomposite films. Macromolecules 2006;39(11):3855–64.
[21] Sinha Ray S, Okamoto M. Polymer/layered silicate nanocomposites: a review from preparation to processing. Prog Polym Sci 2003;28:1539–641.
[22] Manoudis P, Papadopoulou S, Karapanagiotis I, Tsakalof A, Zuburtikudis I, Panayiotou C. Polymer-silica nanoparticles composite films as protective coatings for stone-based monuments. J Phys: Conf Ser 2007;61:1361–5.
[23] Leung CKY, Zhu H-G, Kim J-K, Woo RSC. Use of polymer/organoclay nanocomposite surface treatment as water/ion barrier for concrete. J Mater Civ Eng ASCE 2008;7:484–92.
[24] Woo RSC, Zhu H, Chow MMK, Leung CKY, Kim J-K. Barrier performance of silane–clay nanocomposite coatings on concrete structure. Compos Sci Technol 2008;68:2828–36.
[25] D'Arienzo L, Scarfato P, Incarnato L. New polymeric nanocomposites for improving the protective and consolidating efficiency of tuff stone. J Cultural Heritage 2008;9:253–60.
[26] Scarfato P, Incarnato L. Applications of polymeric treatments in improving building construction materials durability. In: Doyle SG, editor. Construction and building: design, materials, and techniques. NY: Nova Science Publishers; 2010 [Chapter 3].
[27] Hu CG, Kim JK. Epoxy-organoclay nanocomposites: morphology, moisture absorption behavior and thermo-mechanical properties. Compos Interface 2005;12:271–89.
[28] Carmona-Quiroga PM, Martínez-Ramírez S, Sobrados I, Blanco-Varela MT. Interaction between two anti-graffiti treatments and cement mortar (paste). Cem Concr Res 2010;40(5):723–30.
[29] Italian Standard UNI EN 1015-18:2004. Metodi di prova per malte per opere murarie – determinazione del coefficiente di assorbimento d'acqua per capillarità della malta indurita.
[30] Martys NS, Ferraris CF. Capillary transport in mortars and concrete. Cem Concr Res 1997;27(5):747–60.
[31] Kumara R, Bhattacharjeeb B. Assessment of permeation quality of concrete through mercury intrusion porosimetry. Cem Concr Res 2004;34:321–8.
[32] Okamoto M, Ray SS. Polymer/clay nanocomposites. In: Nalwa HS, editor. Encyclopedia of nanoscience and nanotechnology, vol. 8. American Scientific Publishers; 2004. p. 791–843.
[33] Diaconu G, Paulis M, Leiza JR. Towards the synthesis of high solids content waterborne poly(methyl methacrylate-co-butyl acrylate)/montmorillonite nanocomposites. Polymer 2008;49(10):2444–54.
[34] Bharadwaj RK. Modeling the barrier properties of polymer-layered silicate nanocomposites. Macromolecules 2001;34:9189–92.
[35] Ioannou I, Andreou A, Tsikouras B, Hatzipanagiotou K. Application of the sharp front model to capillary absorption in a vuggy limestone. Eng Geol 2009;105:20–3.
[36] Ioannou I, Hamilton A, Hall C. Capillary absorption of water and n-decane by autoclaved aerated concrete. Cem Concr Res 2008;38:766–71.
[37] Bortolotti V, Camaiti M, Casieri C, De Luca F, Fantazzini P, Terenzi C. Water absorption kinetics in different wettability conditions studied at pore and sample scales in porous media by NMR with portable single-sided and laboratory imaging devices. J Magn Reson 2006;181:287–95.
[38] Busscher HJ, Van Pelt AWJ, De Boer P, De Jong HP, Arends J. The effect of surface roughness of polymers on measured contact angles of liquids. Colloids Surf 1984;9:319–31.